

Supporting Information

Trimethylamine Borane: A New Single-Source Precursor for Monolayer h-BN Single Crystals and h-BCN Thin Films

Roland Yingjie Tay,^{1,2,¶} Hongling Li,^{1,3,¶} Siu Hon Tsang,² Minmin Zhu,^{1,3} Manuela Loeblein,^{1,3}
Lin Jing,⁴ Fei Ni Leong,¹ Edwin Hang Tong Teo,^{1,4,*}

¹ School of Electrical and Electronic Engineering, Nanyang Technological University, 50
Nanyang Avenue, Singapore 639798, Singapore

² Temasek Laboratories@NTU, 50 Nanyang Avenue, Singapore 639798, Singapore

³ CNRS-International NTU Thales Research Alliance CINTRA UMI 3288, Research Techno
Plaza, 50 Nanyang Drive, Singapore 637553, Singapore

⁴ School of Materials Science and Engineering, Nanyang Technological University, 50 Nanyang
Avenue, Singapore 639798, Singapore

¶ These two authors contribute equally to this work.

* *Corresponding author.* Tel: +65 67906371. E-mail address: HTTEO@ntu.edu.sg.

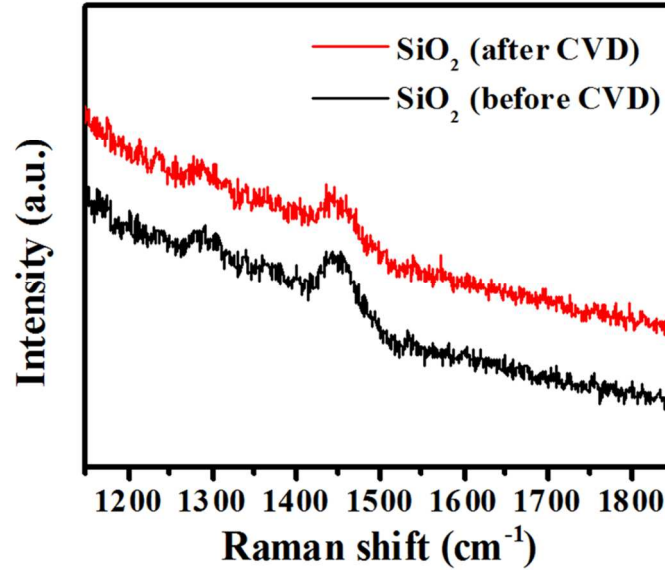


Figure S1. Raman spectra of the as-prepared samples before (black trace) and after (red trace) h-BN CVD growth process on SiO₂ substrates using TMAB as the precursor. The peak at ~1450 cm⁻¹ is attributed to the third order Si transverse optical (TO) phonon mode.¹ No other peak is detected indicating that no film is grown on the SiO₂ surface after CVD process.

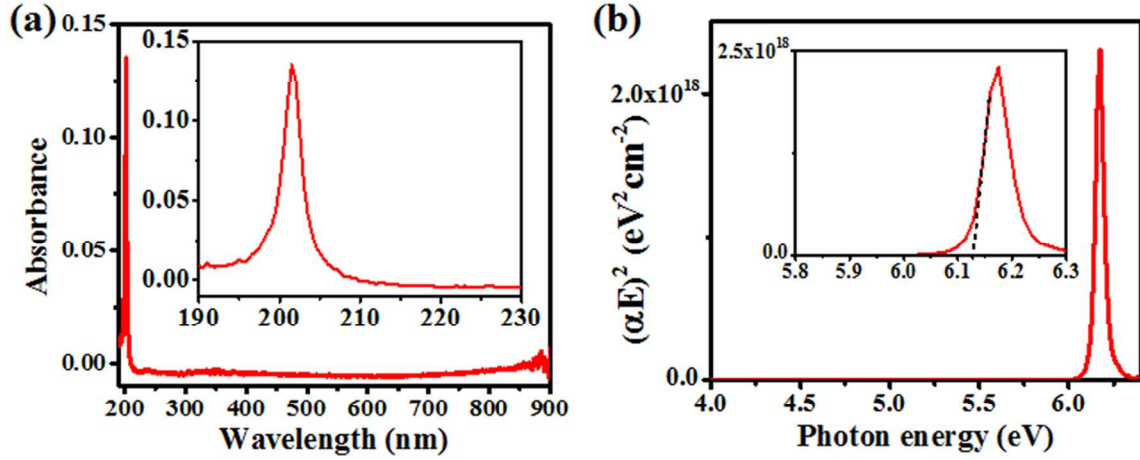


Figure S2. (a) Absorbance spectrum and its corresponding (b) Tauc's plot for OBG extraction of the monolayer h-BN.

Using the derived formula for direct band gap semiconductor,²

$$\alpha = C(E - E_g)^{1/2}/E \quad (1)$$

Where α is the absorption coefficient, C is a constant and E is the photon energy. Note that α is obtained from the optical absorption divided by the thickness of the film. Hence, by plotting $(\alpha E)^2$ against E , a straight line can be extrapolated on the energy dispersion curve and E_g can be extracted from the intersection of the extrapolated line and the x-axis.

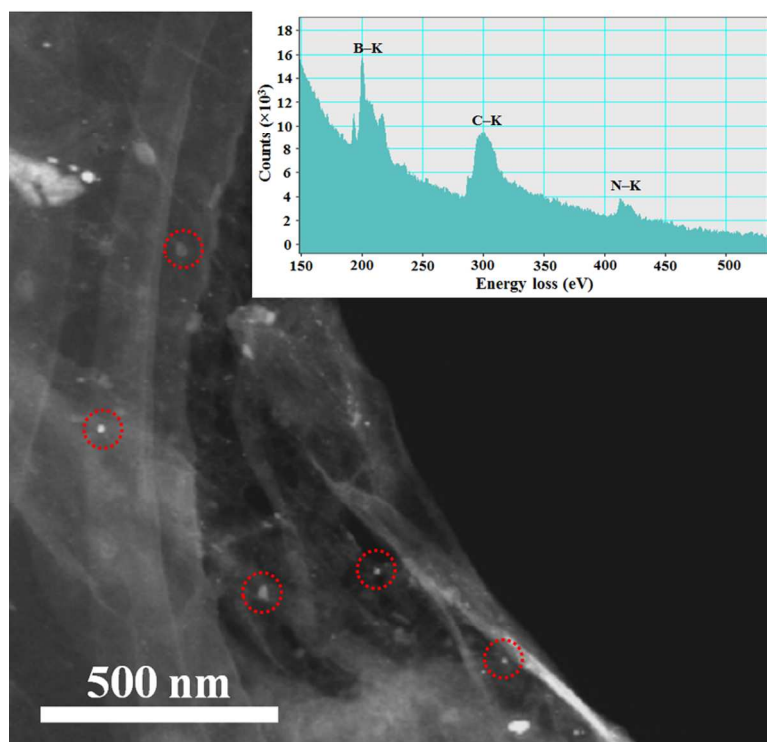


Figure S3. TEM image of a transferred h-BN film with several BN nanoparticles. The inset shows the representative EELS spectrum taken from a BN nanoparticle.

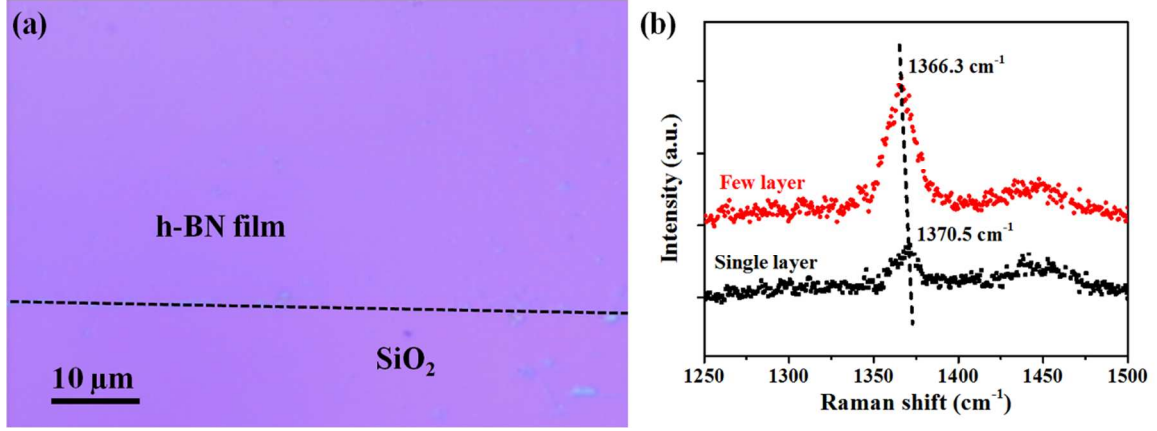


Figure S4. (a) Optical image of the transferred continuous h-BN film. (b) Representative Raman spectra of a monolayer (black trace) and few-layer (red trace) h-BN.

It is observed that most of the regions correspond to a single layer h-BN with a Raman peak at $\sim 1370 \text{ cm}^{-1}$. However, there are several adlayer regions (which are difficult to be identified under our optical scope) where the Raman peak exhibited a relatively higher intensity and slightly downshifted to $\sim 1366 \text{ cm}^{-1}$. According to the reported reference, the h-BN in these regions can be interpreted as few- to multi-layer h-BN.³

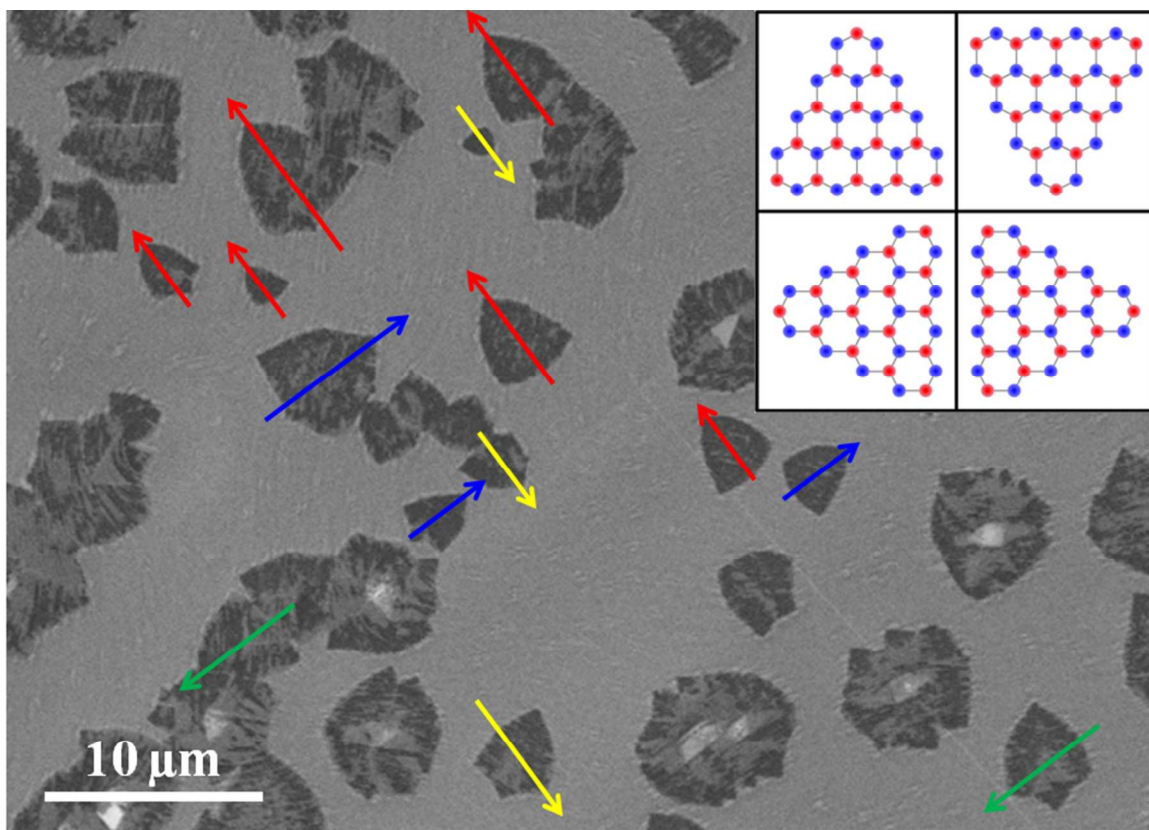


Figure S5. SEM image of h-BN single-crystal domains on polished Cu. The red, yellow, blue and green arrows represent the relative orientations of the domains.

The four orientations can be briefly described by simple geometric representations as shown in the inset. The blue and red spheres represent N and B atoms, respectively. In the SEM image, the (red and yellow) and (blue and green) arrows correspond to 180° mirroring domains (equivalent to 60° rotation in a h-BN unit cell), suggesting that the h-BN domains follow a strict epitaxial relationship with the Cu lattice.^{4,5}

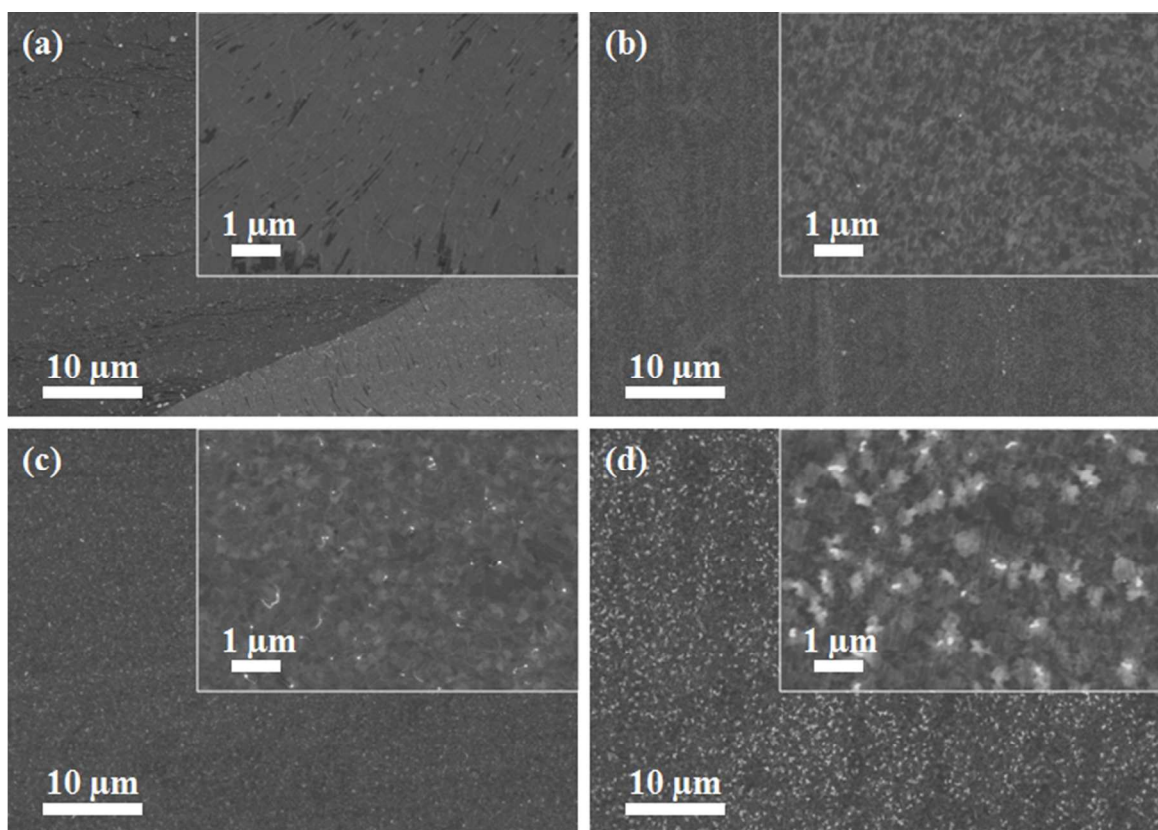


Figure S6. SEM images of as-grown full coverage (a) BN40, (b) BCN50, (c) BCN60 and (d) BCN70 films on Cu.

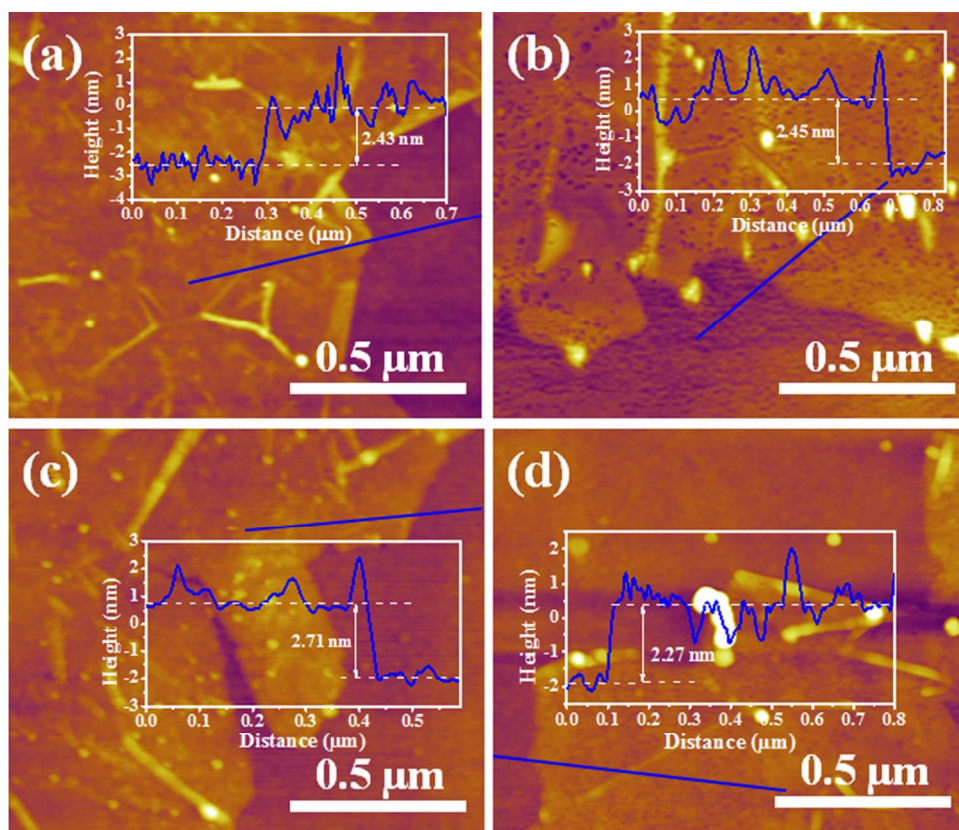


Figure S7. AFM images with their corresponding height profiles (insets) measured across the blue line of the transferred (a) BN40, (b) BCN50, (c) BCN60 and (d) BCN70 films on SiO₂/Si substrates.

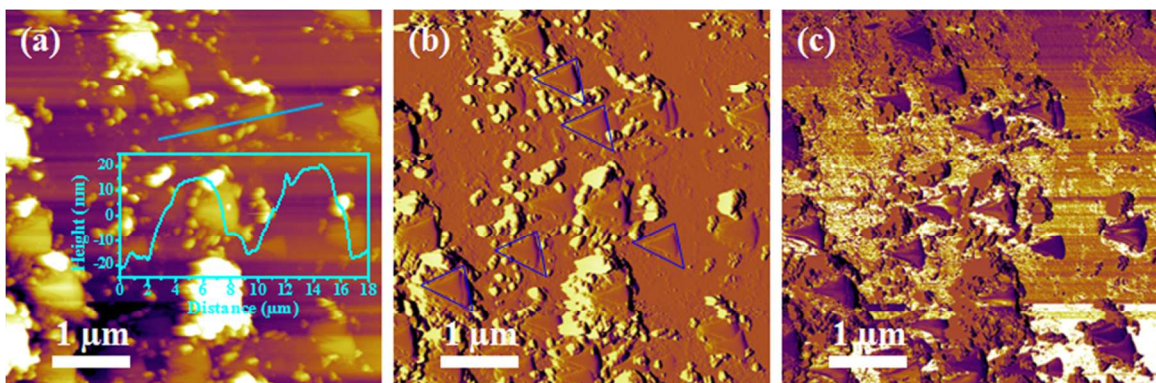


Figure S8. AFM (a) height, (b) amplitude and (c) phase images of a rough film grown at a T_s of 80 °C. Several submicron-sized triangular shaped multilayer islands reaching ~ 30 μm in height can be observed in the film, suggesting the presence of h-BN multilayer.⁶

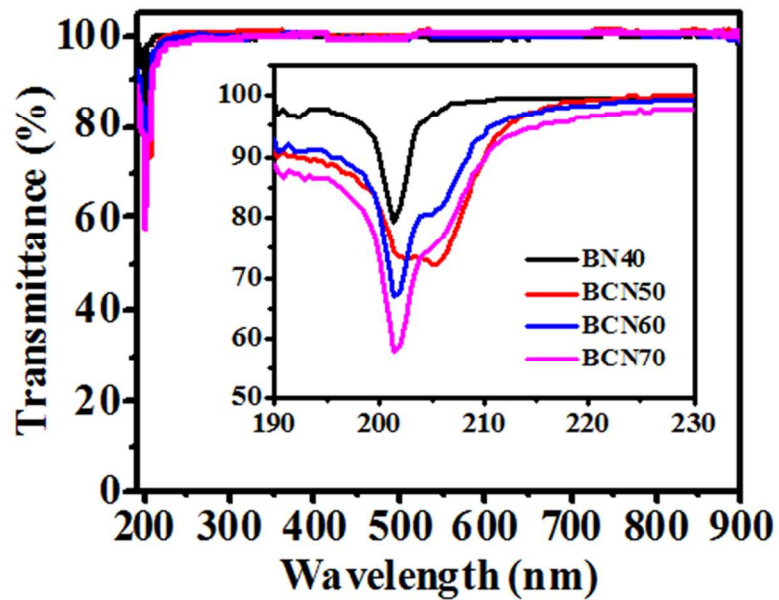


Figure S9. Transmittance spectra of the BN40, BCN50, BCN60 and BCN70 films. The inset shows a magnified plot within the deep UV region. The films are highly transparent throughout the IR and visible spectra.

REFERENCES

1. Spizzirri, P. G.; Fang, J.-H.; Rubanov, S.; Gauja, E.; Prawer, S. Nano-Raman Spectroscopy of Silicon Surfaces. *arXiv:1002.2692v1* **2010**.
2. Yuzuriha, T. H.; Hess, D. W. Structural and Optical Properties of Plasma-Deposited Boron Nitride Films. *Thin Solid Films* **1986**, 140, 199–207.
3. Gorbachev, R. V.; Riaz, I.; Nair, R. R.; Jalil, R.; Britnell, L.; Belle, B. D.; Hill, E. W.; Novoselov, K. S.; Watanabe, K.; Taniguchi, T.; Geim, A. K.; Blake, P. Hunting for Monolayer Boron Nitride: Optical and Raman Signatures. *Small* **2011**, 7, 465–648.
4. Liu, L.; Siegel, D. A.; Chen, W.; Liu, P.; Guo, J.; Duscher, G.; Zhao, C.; Wang, H.; Wang, W.; Bai, X.; McCarty, K. F.; Zhang, Z.; Gu, G. Unusual Role of Epilayer–Substrate Interactions in Determining Orientational Relations in van der Waals Epitaxy. *Proc. Natl. Acad. Sci. U. S. A.* **2014**, 111, 16670–16675.
5. Wood, E. G.; Marsden, J. A.; Mudd, J. J.; Walker, M.; Asensio, M.; Avila, J.; Chen, K.; Bell, R. G.; Wilson, R. N. van der Waals Epitaxy of Monolayer Hexagonal Boron Nitride on Copper Foil: Growth, Crystallography and Electronic Band Structure. *2D Mater.* **2015**, 2, 025003.
6. Kim, K. K.; Hsu, A.; Jia, X.; Kim, S. M.; Shi, Y.; Hofmann, M.; Nezich, D.; Rodriguez-Nieva, J. F.; Dresselhaus, M.; Palacios, T.; Kong, J. Synthesis of Monolayer Hexagonal Boron Nitride on Cu Foil using Chemical Vapor Deposition. *Nano Lett.* **2012**, 12, 161–166.